VORTICITY MOMENTS FOR THIN AND HOLLOW ANTI-PARALLEL VORTEX TUBES

Robet M. Kerr
Department of Mathematics, University of Warwick, Coventry, UK

Abstract New mathematics, numerical analysis and graphics are applied to the interaction of very long and relatively thick anti-parallel vortex tubes with respect to discerning whether either the Euler or Navier-Stokes equations might have singularities. Preliminary results that were largely consistent with existing singular behaviour for the Euler equations was the basis of the original submission to ETC-14 and to J. Fluid Mechanics. The final conclusions are different, with a transition from singular to super-exponential growth appearing as the helicity and torsion of the vortex lines grows and resists singular growth. The numerical analysis is based upon new mathematics that uses a rescaling of the vorticity moments that allows us to compare all orders between the two extremes, the maximum of vorticity and enstrophy. The original mathematics was designed for the Navier-Stokes equations, with anti-parallel simulations finding a hierarchy that is the opposite of the usual Hölder ordering of these moments [1]. This ordering has since been found in every high-Reynolds number simulation it has been tested against [3] and is obeyed for a surprisingly long period in the simulations of the Euler equations discussed here. When, eventually, the Euler solutions break this hierarchy and becomes super-exponential, a high-Reynolds number Navier-Stokes calculation with the same initial condition, continues to obey the hierarchy, even if it is not singular as the growth of the D_m stops. This raises the question of whether the Euler equations are the proper $\nu \to 0$ limit of the Navier-Stokes equations.

RESCALING OF VORTICITY MOMENTS

The following rescaled viscous vorticity moments [4] have been used on anti-parallel vortex tubes simulated by Navier-Stokes [1] and Euler [2].

$$\Omega_m = \left(L^{-3} \int_{\mathcal{V}} |\omega|^{2m} dV \right)^{1/2m} \quad \text{into} \quad D_m = (\varpi_0^{-1} \Omega_m)^{\alpha_m} \tag{1}$$

where $\varpi_0 = \varpi_\nu = \nu/\mathsf{L}^2$ for Navier-Stokes, $\varpi_0 = \varpi_\Gamma = \Gamma/\mathsf{L}^2$ for Euler and $\alpha_m = 2m/(4m-3)$ with Γ the circulation about the vortices and L the size of the domain perpendicular to the vortices L_z.
For all times and for all turbulent simulations they have been applied to [3], the D_m are ordered as $D_m > D_{m+1}$, not the ordering required for the raw moments, which is $\Omega_{m+1} > \Omega_m$. This is demonstrated in the first figure where for all times the $D_m^{-2} < D_{m+1}^{-2}$.
The new calculations use very long anti-parallel vortices with balanced core profiles and the perturbation to their trajectories is localised far from boundaries [1]. The dealiased, truncated pseudospectral numerical method takes advantage of the the symmetries in the vortical and spanwise directions with the largest calculations being the order of $1024 \times 1024 \times 4096$ points.
To most clearly see possible singular behaviour, one plots D_m^{-2} because $D_m^2 \sim \|\omega\|_\infty \sim 1/(T_c - t)$ is the lower limit of possible singular behaviour allowed by taking the time integral of the maximum of vorticity $\|\omega\|_\infty$. In this way, it can be seen that for $m > 1$ all the $D_m^{-2} \to (T_c - t)$. The exception is $m = 1$, the enstrophy $Z = \Omega_1^2 \sim D_1$. Also note that for all m for $t > 13$, the trend is to break this hierarchy, as shown by the inset in Fig.1. As in earlier work, the enstrophy growth appears to be logarithmic $Z \sim D_1 \sim -\log(T_c - t)$, and the persistence of this behaviour is the first sign that the new hierarchy in Euler eventually breaks down and some type of non-singular behaviour might form. The thin and hollow vortex simulations shown in the original abstract did not support singular growth as hoped, but showed the transition away from such growth more strongly than the thick vortex simulations here.
To understand the transition away from singular-like growth , the following inequality for the Euler equations is used [4, 2].

$$-\frac{d}{dt} D_m^{-2} \le c_{2,m} \varpi_\Gamma \left(\frac{D_{m+1}}{D_m} \right)^{\xi_m} \tag{2}$$

By comparing the left and right-hand sides of this inequality, the reason for singular growth for intermediate times can be seen, as well as the first signs that the hierarchy is breaking down for these Euler solutions. The final growth of all the Ω_m Euler moments is super-exponential growth [2].

References

[1] R.M., Kerr Swirling, turbulent vortex rings formed from a chain reaction of reconnection events *Phs. Fluids* **25**: 065101, 2013a.
[2] R.M., Kerr Bounds for Euler from vorticity moments and line divergenced. *J. Fluid Mech.* : In press, 2013b.
[3] D., Donzis, J.D., Gibbon, KERR, R. M., PANDIT, R., GUPTA, A., & VINCENZI., D. 2013 Rescaled vorticity moments in the 3D Navier-Stokes equations. arXiv:1302.1768v1.
[4] J.D., Gibbon Dynamics of scaled norms of vorticity for the three-dimensional Navier-Stokes and Euler equations *Procedia IUTAM* **7**: 49–58, 2013.

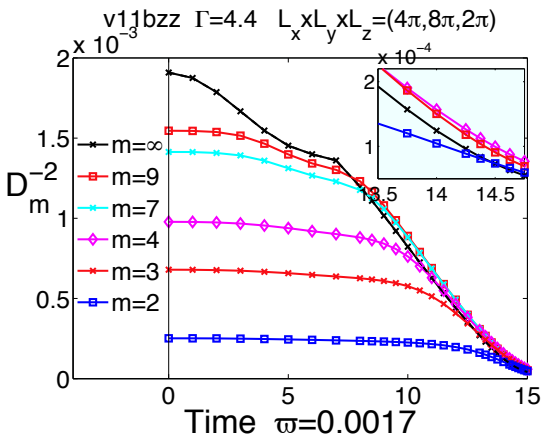

Figure 1. The inverses: $D_m^{-2}(t)$. Common linear decrease for $m > 1$ shows strong, convergent growth for the D_m for $t \leq 13.75$. The hierarchy of $D_m^{-2}(t)$ includes $\varpi/\|\boldsymbol{\omega}\|_\infty$. The inset shows the D_m^{-2} crossing for large m, which is not seen for the large m Navier-Stokes D_m^{-2} [2].

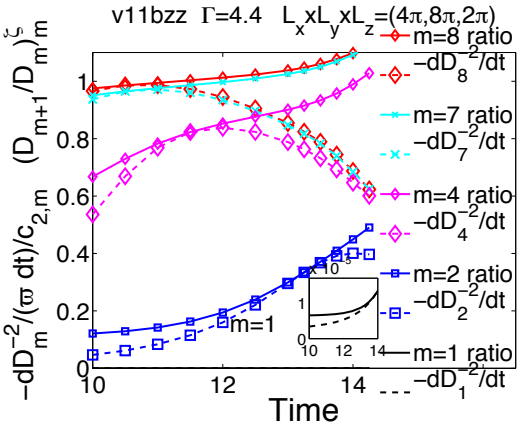

Figure 2. Comparison using (2) of $dD_m^{-2}/dt(c_{2,m}\varpi_\Gamma)^{-1}$ to $(D_{m+1}/D_m)^{\xi_m}$ for case v11bzz. Singular-like growth could exist if $(D_{m+1}/D_m)^{\xi_m} \leq 1$ and $dD_m^{-2}/dt(c_{2,m}\varpi_\Gamma)^{-1} \sim (D_{m+1}/D_m)^{\xi_m}$ These bounds are followed for $t < 11$. For $t > 11$, $(D_{m+1}/D_m)^{\xi_m}$ rises above 1 and dD_m^{-2}/dt diverges from this bound for large m, showing a transition to a new regime. The growth rate in the new regime is an exponential of an exponential [2].

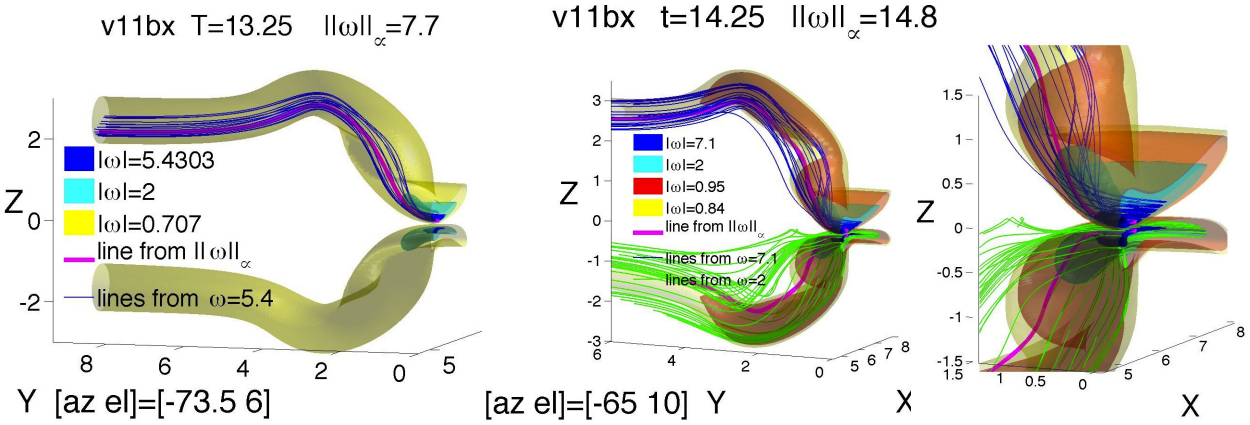

Figure 3. The goal of these figures is to demonstrate the growth of helical and divergent vortex patterns, which tend to suppress nonlinearities. Isosurfaces and vortex lines are shown in the $y > 0$ half-domain, where the $\pm z$ vortices are mirror images. Thick, magenta lines originate at $\|\omega\|_\infty$. Yellow, outer isosurfaces show the overall envelope. Blue isosurfaces show the region immediately around $\|\omega\|_\infty$. **Left:** $t = 13.25$ with three isosurfaces. Two show the structure around $\|\omega\|_\infty$. The outer envelope surface shows how the strongly interacting region near $y = 0$ connects to the original vortices, with some twist on the way. The blue vortex lines coming from the $|\omega| = 0.7\|\omega\|_\infty$ isosurface stay bundled, except for some divergence when they cross $y = 2$. **Center and Right:** $t = 14.25$ shows four isosurfaces with more twist and distorsion. Two surfaces represent the innermost region, an intermediate surface (red) is the most convoluted, plus the yellow envelope surface. The inner vortex lines (magenta and blue) remain bundled, with more spreading than at $t = 13.25$ near $y = 2$, where isosurfaces are most convoluted. The green vortex lines originating on the $y = 0$, $|\omega| = 2$ isosurface are more spread out and twisted than the inner lines, with a twist that brings one close to the $z = 0$ dividing plane near $y = 2$, which could enhance the local stretching rate.